Development and Implementation of New Triangular Finite Element in ABAQUS for Linear, Nonlinear and Free Vibration Problems

Lahcen Fortas[1], Houssam Eddine Khiouani[2], Abderraouf Messai[3], Lamine Belounar[4], Tarek Merzouki[5]

[1]Technology Department, Higher Normal School of Technological Education of Skikda, Skikda, Algeria

[2]MN2I2S Laboratory, Faculty of Science and Technology, Biskra University, Algeria

[3]Department of Civil Engineering, University Ferhat Abbas SETIF 1, SETIF, Algeria

[4]MN2I2S Laboratory, Faculty of Science and Technology, Biskra University, Algeria

[5]LISV, University of Versailles Saint-Quentin, 10-12 Avenue de l'Europe, 78140 Vélizy, France

Received: **05/2023**, Published: **07/2023**

Abstract

Purpose – A new triangular membrane finite element based on the strain approach is developed for the linear, nonlinear and free vibration analysis.

Design/methodology/approach – The current element has two degrees of freedom at each of the three corner nodes and the internal node (two translations) and satisfies the exact representation of the rigid body modes of displacements.

Findings - The displacements field of the element has been developed by the use of the strain-based approach and it based on the assumed independent functions for the various components of strain satisfying the compatibility equations.

Originality/Value – The developed element is implemented in the ABAQUS code using the UEL subroutine (User Element subroutine of ABAQUS). For elastoplastic analysis, Von Mises and Mohr–Coulomb yield criteria are adopted. Several numerical tests were performed, including linear, nonlinear and free vibration problems. The results obtained were compared to the available analytical and numerical solutions. It turned out that the use of this element allows acquiring effective convergence and accurate results.

Keywords: strain approach; membrane; linear analysis; nonlinear analysis; free vibration analysis

Paper type: Research paper.

Tob Regul Sci. ™ 2023;9(1): 3561-3576
DOI: doi.org/10.18001/TRS.9.1.248

1. Introduction

The strain-based approach was an important area where researchers worked on the development of new finite elements. Several researchers have used this approach to formulate robust elements. The displacement field can be obtained by direct integration of the imposed strains field contrary to the conventional displacement model. The first applications of this approach that of (Ashwell et al.,1971).for curved problems. This approach was extended to plane elasticity (Sabir.,1985a;

Hamadi et al.,2006). , to problems of three-dimensional elasticity (Belarbi et al.,1999; Messai et al.,2019), in shell structures(Sabir et al.,1972; Hamadi et al.,2015), and for bending of plates(Belounar L et al.,2005; Belounar A et al.,2018). The strain-based elements in polar coordinates were also developed by (Sabir.,1985b; Khiouani et al.,2020).

In this paper a new triangular plane elasticity element based on the strain approach with three Corner Nodes and an Internal Node with the two essential external degrees of freedom (U and V) at each node SBT4 (Strain-based Triangular with four Nodes) is proposed to enrich the Library of existing finite elements.

The static, nonlinear and free vibration analyses are considered in a series of test cases of the literature to evaluate its performance. Through these numerical examples, results relating to the quick convergence will also be given, and comparisons will be made with other elements.

The developed element is implemented into ABAQUS using the UEL subroutine (User Element subroutine of ABAQUS)

2. Materials and methods

2.1 Formulation of the displacements field

The strain-displacement relations for plan elasticity element in the Cartesian coordinates system **Figure 1** can be written as:

Figure 1 Triangular strain based element (SBT4)

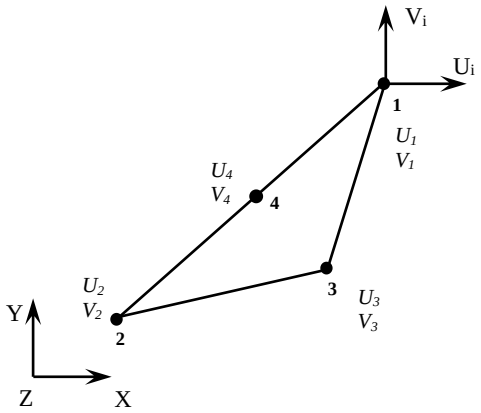

$$\varepsilon_x = \frac{\partial U}{\partial x}$$
$$\varepsilon_y = \frac{\partial V}{\partial y} \qquad (1)$$
$$\gamma_{xy} = \frac{\partial U}{\partial y} + \frac{\partial V}{\partial x}$$

In matrix form, it can be given as:

$$\begin{Bmatrix} \varepsilon_x \\ \varepsilon_y \\ \gamma_{xy} \end{Bmatrix} = \begin{bmatrix} \partial/\partial x & 0 \\ 0 & \partial/\partial y \\ \partial/\partial y & \partial/\partial x \end{bmatrix} \begin{Bmatrix} u \\ v \end{Bmatrix}$$

The strain components are given by equations (1) and must satisfy the compatibility equation which is given as:

$$\frac{\partial^2 \varepsilon_x}{\partial y^2} + \frac{\partial^2 \varepsilon_y}{\partial x^2} - \frac{\partial^2 \gamma_{xy}}{\partial x \partial y} = 0 \qquad (2)$$

The current element SBT4 possesses two degrees of freedom (u, v) at each of the four nodes and therefore the displacement field should contain eight independent constants. First, the resulting displacement fields to the rigid body modes are obtained by equating the three strains given in equations (1) to zero, and after integration, we can obtain:

$$U = a_1 - a_3 y$$
$$V = a_2 + a_3 x \tag{3}$$

Since the three constants (a1, a2 and a3) are taken in the representation of the rigid body modes, the five constants left are used to express the displacement due to straining of the element satisfying the compatibility equation and which is given in equations (4). The assumed strains of the developed element in terms of the five remaining constants (a4, a5, a6, a7, a8) are apportioned as follows:

$$\varepsilon_x = a_4 + a_5 y - a_7 \frac{1}{3} x$$
$$\varepsilon_y = -a_5 \frac{1}{3} y + a_6 + a_7 x$$
$$\gamma_{xy} = a_8$$
(4)

The assumed strains of equations (4) are substituted in equations (1) and the obtained displacements are summed with those of equations (3) to get the final displacement functions given by:

$$u = a_1 - a_3 y + a_4 x + a_5 xy - a_7 (\frac{1}{6} x^2 + \frac{1}{2} y^2) + a_8 y / 2$$
$$v = a_2 + a_3 x - a_5 (\frac{1}{6} y^2 + \frac{1}{2} x^2) + a_6 y + a_7 xy + a_8 x / 2 \tag{5}$$

For developed element SBT4, the displacement function (equations (5)) and the strain functions (equations (4)) can respectively be written in matrix from as:

$$\{U\} = \begin{Bmatrix} u \\ v \end{Bmatrix} = [P]\{a\} \tag{6}$$

$$\{\varepsilon\} = \begin{Bmatrix} \varepsilon_x \\ \varepsilon_y \\ \gamma_{xy} \end{Bmatrix} = [Q]\{a\} \tag{7}$$

With:

$$\{a\} = \{a_1, a_2, ..., a_8\}^T$$

$$[P] = \begin{bmatrix} 1 & 0 & -y & x & xy & 0 & -(\frac{1}{6}x^2 + \frac{1}{2}y^2) & y/2 \\ 0 & 1 & x & 0 & -(\frac{1}{6}y^2 + \frac{1}{2}x^2) & y & xy & x/2 \end{bmatrix} \tag{8}$$

$$[Q]=\begin{bmatrix} 0 & 0 & 0 & 1 & y & 0 & -\frac{1}{3}x & 0 \\ 0 & 0 & 0 & 0 & -\frac{1}{3}y & 1 & x & 0 \\ 0 & 0 & 0 & 0 & 0 & 0 & 0 & 1 \end{bmatrix} \tag{9}$$

The nodal displacements vector {qe} is obtained in terms of the constant parameters vector {a} by applying the relation (5) for each of the four element nodes coordinates (x_i, y_i), (i=1, 2, 3, 4) as:

$$\{q_e\}=[C]\{a\} \tag{10}$$

With:

$$\{q_e\}=\{u_1,v_1,u_2,v_2,u_3,v_3,u_4,v_4\}^T$$

And the transformation matrix [C] is:

$$[C]=\begin{bmatrix} [P(x_1,y_1)] \\ [P(x_2,y_2)] \\ [P(x_3,y_3)] \\ [P(x_4,y_4)] \end{bmatrix} \tag{11}$$

The constant parameters vector {a} can be derived from equations (10) as follow:

$$\{a\}=[C]^{-1}\{q_e\} \tag{12}$$

By substituting equations (12) into equations (6) and (7) we obtain:

$$\{U\}=[P][C]^{-1}\{q_e\}=[N]\{q_e\} \tag{13}$$

$$\{\varepsilon\}=[Q(x,y)][C]^{-1}\{q_e\}=[B]\{q_e\} \tag{14}$$

With:

$$[N]=[P][C]^{-1};\quad [B]=[Q(x,y)][C]^{-1} \tag{15}$$

The stress-strain relationship is given by:

$$\{\sigma\}=[D]\{\varepsilon\} \tag{16}$$

Where the elasticity matrix [D] is given in appendix A for plane stress and plane strain.
The standard weak form for static and free vibration can respectively be expressed as:

$$\int_{V^e}\delta\{\varepsilon\}^T\{\sigma\}dV=\int_{V^e}\delta\{U\}^T\{f_v\}dV \tag{17}$$

$$\int_{V^e}\delta\{\varepsilon\}^T\{\sigma\}dV+\int_{V^e}\delta\{U\}^T\{\ddot{U}\}dV=0 \tag{18}$$

By substituting equations. (13), (14) and (16) into equations (17) and (18) we obtain:

$$\delta\{q_e\}^T\left(\int_V [B]^T[D][B]dV\right)\{q_e\} = \delta\{q_e\}^T\left(\int_V [N]^T\{f_v\}dV\right) \tag{19}$$

$$\delta\{q_e\}^T\left(\int_V [B]^T[D][B]dV\right)\{q_e\} + \delta\{q_e\}^T\left(\int_V \rho[N]^T[N]dV\right)\{\ddot{q}_e\} = 0 \tag{20}$$

Where the element stiffness {Ke} and mass {Me} matrices are respectively as:

$$[K_e] = \int_V [B]^T[D][B]dV = [C]^{-T}\left(\int_V [Q]^T[D][Q]dV\right)[C]^{-1} \tag{21}$$

$$[M_e] = \int_{V_e} \rho[N]^T[N]dV = [C]^{-T}\left(\int_{V_e} [P]^T[P]dV\right)[C]^{-1} \tag{22}$$

And the element nodal body forces vector is:

$$\{F_b\} = \int_{V_e} [N]^T\{f_v\}dV = [C]^{-T}\left(\int_{V_e} [P]^T\{f_v\}dV\right) \tag{23}$$

After assembly over all elements, the global stiffness and mass matrices {K}, {M} are used in global equations for static and free vibration given as:

$$[K]\{q\} = [F] \tag{24}$$

$$[K] - \omega_k^2[M]\{q\} = 0 \tag{25}$$

3. Results and discussion

3.1 Linear tests

3.1.1 Linear Mac-Neal beam

In this test, the problem of a slender Mac-Neal beam ([27]) shown in Figure 2 is considered for testing the sensitivity to mesh distortion. This analysis is considered as a test of a thin beam with shear in the plane and out of the plane, a tensile force and a constant bending moment. Three different mesh shapes, rectangular, trapezoidal and parallelogram are considered.

Figure 2 Mac-Neal's elongated beam subjected to end shear (1) and end bending (2)

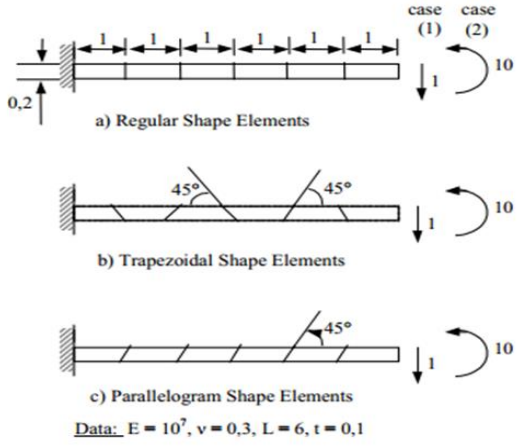

The obtained results presented in Table 1 show that the developed element is insensitive to mesh distortion and are in good agreement with the exact solution for all loading types and all mesh shapes for the reason that it is free for any blocking phenomenon.

Table 1 Normalized deflection at free end for Mac-Neal's elongated beam subjected to end shear and bending

Element	Bending			End shear		
	Regular	Trapezoidal	Parallel	Regular	Trapezoidal	Parallel
Q4	0,093	0,022	0,031	0,093	0,027	0,034
PS5β (macNealet al.,1985)	1,000	0,046	0,726	0,993	0,052	0,632
AQ (Pian et al.,1984)	0,910	0,817	0,881	0,904	0,806	0,873
MAQ (Cook.,1986)	0,910	0,886	0,890	0,904	0,872	0,884
Q4S (Yanus et al.,1989)	-	-	-	0,993	0,986	0,988
07β (Mc Neal et al.,1988)	1,000	0,998	0,992	0,993	0,988	0,985
SBT2V (Belarbi et al.,2005)	0,948	0,952	0,944	0,944	0,833	0,874
SBTIEIR (Sabir .,1985a)	0.437	0.015	0.374	0.435	0.005	0.333
CPS4	0,093	0,022	0,031	0,093	0,027	0,034
SBT4	**1.000**	**1.000**	**1.000**	**0.993**	**0.993**	**0.993**
BeamTheory		**1,000 (0,270)**			**1,000 (0,1081)**	

3.1.2 Short cantilever beam under shear force

The second test is a short homogeneous cantilever beam, which is subjected to a parabolic shear force at its free end. The other end is fixed whose nodal displacements on this side are set to zero.

The exact deflection of the free end is equal to 0.35601 (Szek et al.,1992) (Table 2). Figure 3 shows the geometry of the beam whose length is 48, a height is 12 with a width of 1. The modulus of elasticity is equal to 30000 and the Poisson's ratio is 0.25. All the associated values in this example are dimensionless. The total shear load acting on the beam is 40.

We remark that the present element SBT4 behaves almost as CPS6 and accurate quickly to the reference solution.

Figure 3 Short cantilever beam under shear force

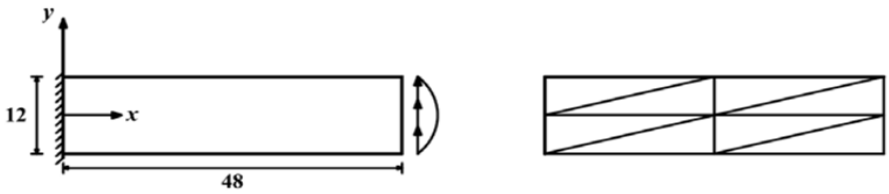

Table 2 Normalized vertical displacement at the free end of the beam

	Mesh			
Element	2×2	4×4	8×8	16×16
MEAS [34]	17.94	43.92	75.05	92.17
Allman	52.25	66.61	87.91	96.44
OPT	91.06	96.00	98.23	99.27
CST Hybrid	74.34	91.49	97.38	99.22
SM3	92.76	97.14	98.89	99.60
CPS3	18.02	43.99	75.14	92.27
CPS6	96.26	99.32	99.97	100.25
SBT4	91.88	97.50	99.32	99.97

3.1.3 Thick circular beam under in-plane shear load

In this test, a thick circular beam subjected to a shear force F = 600 at its free end is considered (Figure 4). Four regular meshes of 2x1, 4x1, and 6x1 plane stress quadrilateral elements for this curved beam are used. The obtained results of the vertical displacement at point A are given in Table 3 and compared with those of other elements which show that the developed element gives more accurate results than the CPS3 element.

Figure 4 Thick circular beam modeled with 4x1 triangular elements

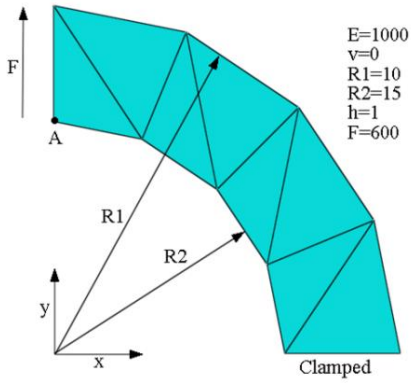

Table 3. Normalized vertical displacement at point A (reference solution = 90.1)

Mesh	CPS4	CPS3	SBT4
2x1	0.251	0.118	0.496
4x1	0.643	0.244	0.638
6x1	0.811	0.295	0.682

3.1.4 Thin circular beam under in-plane shear load

The test shown in Figure 5 concerns the thin circular beam fixed at one end and subjected to a unit shear load at the other end.

Three regular meshes of 6x1 and 12x2 plane stress quadrilateral elements are considered. The obtained results of the vertical displacement at point A are given in Table 4, the vertical displacement at point A and the near-exact vertical displacement is equal to 0.08734 (Felippa .,2003). It can be seen that the SBT4 element offers a better convergence towards the exact solution compared to the other elements.

Figure 5 thin circular beam modelled with 6x1 triangular elements

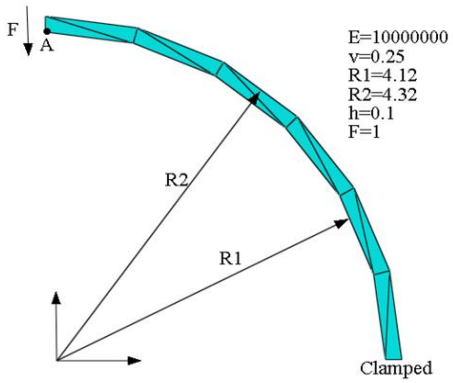

Table 4. Normalized vertical displacement at point A

Mesh	CPS4	HT	CPS3	SBT4
6x1	0.073	0.075	0.025	0.31
12x2	0.247	0.251	0.095	0.53

3.2 Free vibration numerical validation

Three problems are presented to demonstrate the robustness and accuracy of the present element for free vibration analysis.

3.2.1 Free vibration analysis of cantilever beam

In this example, we study a plane stress cantilever beam with geometrical and mechanical characteristics given in Figure 6.

Figure 6 Meshes of the cantilever beam

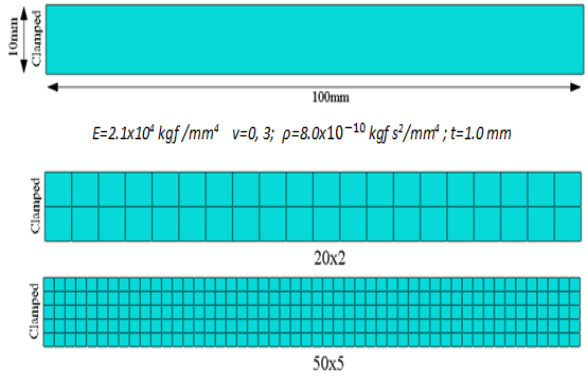

Table 5 summarize the four first frequencies and their corresponding modes shapes are depicted in Figure 7. We remark that results demonstrate satisfactory convergence of the present element SBT4 when compared to other elements.

Figure 7 The first four natural modes of cantilever beam

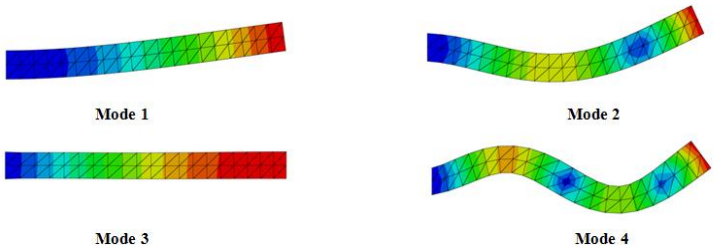

Table 5. First four natural frequencies (x104 Hz) of a cantilever beam

element	SFEM (4SC) [35]	FEM (8-nodeQ9) [35]	FEM (4-nodeQBI) [35]	CPS4	CPS3	CPS6	SBT4
10X1	0.0861	0.0827	0.0817	0.1000	0.1691	0.0826	0.0819
	0.5071	0.4982	0.4824	0.6077	0.9162	0.4997	0.4876
	1.2828	1.2832	1.2526	1.2863	1.2869	1.2834	1.2660
	1.3124	1.3205	1.2826	1.6423	2.1843	1.3311	1.2928

20X2	0.0834	0.0823	0.0822	0.0872	0.1117	0.0823	0.0823
	0.4993	0.4940	0.4928	0.5264	0.6539	0.4941	0.4942
	1.2828	1.2827	1.2827	1.2837	1.2843	1.2827	1.2823
	1.3141	1.3020	1.2982	1.4011	1.6748	1.3032	1.3052
50X5	0.0824	0.0822	0.0822	0.0831	0.0877	0.0822	0.0822
	0.4944	0.4934	0.4934	0.4989	0.5245	0.4933	0.4935
	1.2825	1.2825	1.2825	1.2827	1.2829	1.2824	1.2825
	1.3024	1.2997	1.2998	1.3168	1.3766	1.2995	1.3008
100X10	0.0823	_	0.8222	0.0824	0.0836	0.0822	0.0822
	0.4935	_	0.4933	0.4947	0.5014	0.4932	0.4933
	1.2824	_	1.2824	1.2825	1.2826	1.2824	1.2824
	1.3000	_	1.2993	1.3037	1.3196	1.2992	1.2996

3.2.2 Free vibration analysis of a variable cross-section beam

In this part, a cantilever beam with a variable cross-section is considered. The Figure 8 shows the geometrical and mechanical characteristics. The results obtained of the first four natural frequencies for the SBT4 element are resumed in Table 6 which shows that this element has similar behaviour as CPS4 and CPS6 elements.

The figure 9 present the corresponding modes shape of the first four natural frequencies.

Figure 8 Cantilever beam with variable cross-section and its meshes

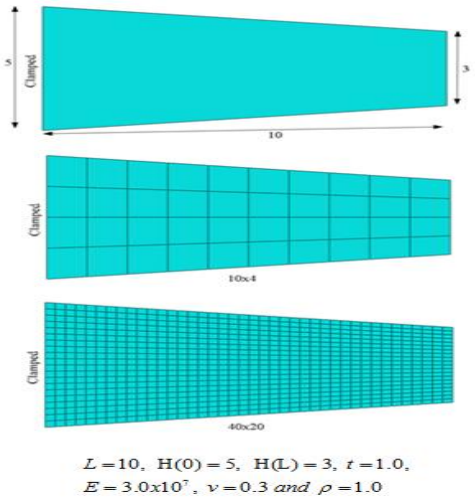

Figure 9 The first four natural modes of cantilever beam with variable cross-section

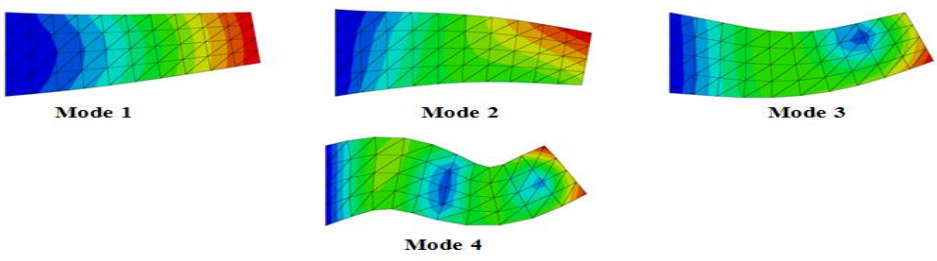

Table 6. First four natural frequencies (x103 rad/s) for a cantilever beam with a variable cross-section

Element	CPS4	CPS3	CPS6	SBT4
10X4	0.2618	0.2810	0.2618	0.2609
	0.9188	0.9503	0.9193	0.9177
	0.9522	0.9703	0.9522	0.9518
	1.8557	1.9304	1.8586	1.8440
20X10	0.2621	0.2656	0.2616	0.2615
	0.9189	0.9295	0.9179	0.9151
	0.9519	0.9525	0.9520	0.9547
	1.8509	1.8749	1.8528	1.8498
40X20	0.2617	0.2626	0.2616	0.2615
	0.9180	0.9209	0.9177	0.9147
	0.9519	0.9521	0.9520	0.9551
	1.8520	1.8588	1.8523	1.851

3.3 Elasto-plastic analysis

3.3.1 Bearing capacity analysis of purely coherent soil

This example studies a flexible strip footing at the surface of a layer of uniform undrained clay shown in Figure 10. This problem has been treated in (Dai et al.,2007), by the use of the 8-node quadrilateral element. The elastoplastic properties of soil is described by three parameters Young's modulus E=105 kN/m2, Poisson's ration v=0.3, and the undrained cohesion Cu=100 kN/m^2. The footing is subjected to a uniform stress of q=1 kN/m2, which gradually increases to failure.

In this test, Plane strain conditions, the visco-plastic method and the Von Mises criterion are assumed. Bearing failure in this problem occurs when reaches the Prandtl load given by $q_{ultime}=(2+\pi)Cu$.

The Figure 11 plot the obtained results in the form of a dimensionless bearing capacity factor q/Cu versus centreline displacement. These results show that the SBT4 element is in good agreement with the quadratic element Q8.

Figure 10 Geometry and mesh of the flexible strip footing

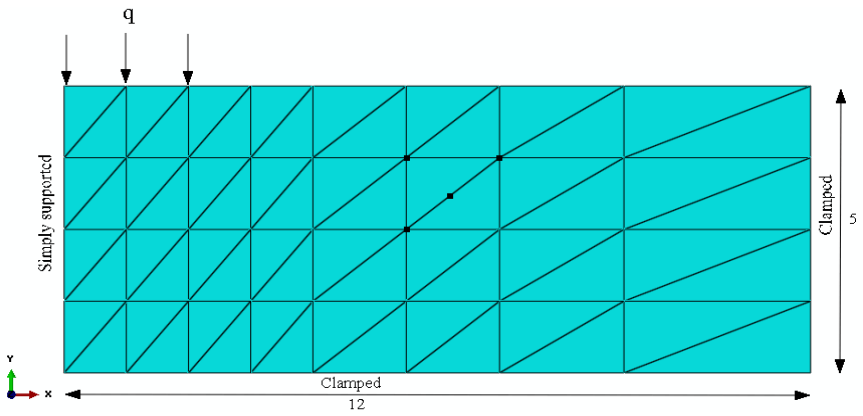

Figure 11 Bearing stress versus centreline displacement

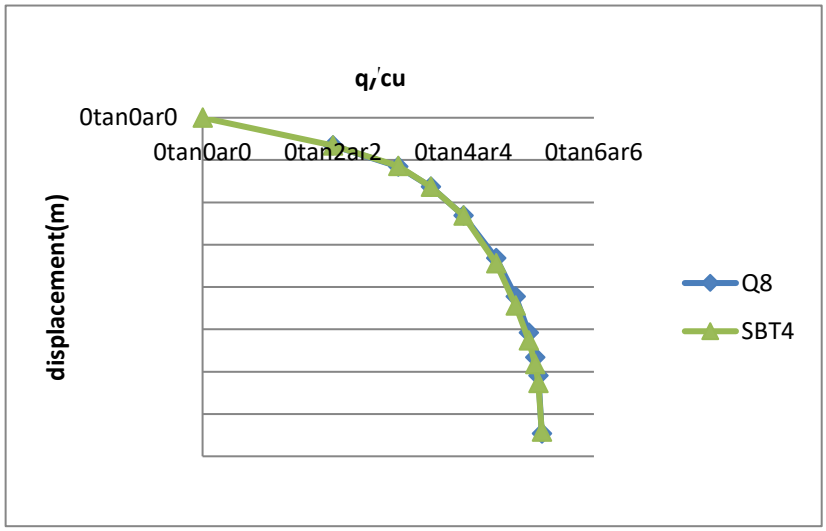

3.3.2 Axisymmetric undrained analysis

Figure 12 represents the assembly of two axisymmetric triangular (SBT4) elements subjected to vertical compressive displacement increments along its top face. The Q8 element was used in this test by Smith et al. (Smith.,14). The analysis is of a triaxial test, in which the sample has been consolidated under a cell pressure of 100 kN/m2, followed by undrained axial loading. Two types of analysis are considered in this problem. In the first case (a) where there is no plastic volume change the dilation angle ψ= 0, and in the second case (b) which includes an associated flow rule (ψ = 30°).

The sample properties for this problem are given in Figure 12. In this problem the visco-plastic method and the Mohr Coulomb criterion were used. The results of the deviatoric stress and the pore pressure with respect to the vertical displacement in the two cases (ψ= 0 and ψ= 30°) are given in Tables 7 and 8.

We note for the first case that the deviatoric stress of the SBT4 element reaches a peak of 119.43 KN/m² which is far compared to the solution given by (Grif.85à which is equal to 120.8 KN/m²; on the other hand the Q8 element is in good agreement with its value of 121 KN/m² (Smi.,14).

For the second case, which includes an associated flow rule (ψ= 30°), it is noticed the absence of any sign of failure (rupture) due to the tendency and the dilation. In this case, it is found that the pore pressures continue to occur and the deviatory stress continues to increase, and this is due to the influence of expansion on the behaviour of the two elements.

Figure 12 Geometry and mesh of the axisymmetric problem

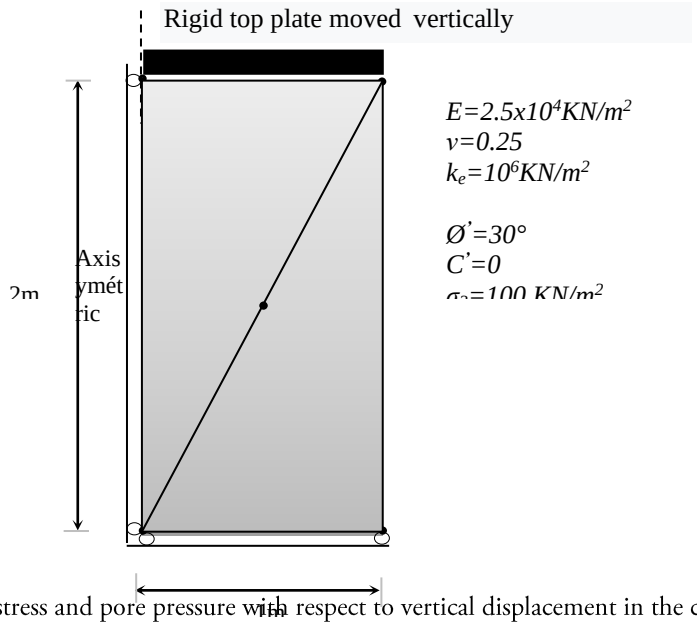

Table 7. Deviator stress and pore pressure with respect to vertical displacement in the case (ψ= 0°).

Displacement	Q8		SBT4	
	Deviator stress	pore pressure	Deviator stress	pore pressure
-0.2000.10-2	29.90	-9.804	29.70	-13.14
-0.4000.10-2	59.80	-19.61	59.40	-26.27
-0.6000.10-2	89.71	-29.41	89.09	-39.41
-0.8000.10-2	119.6	-39.22	101.61	-40.08
-0.1000.10-1	120.9	-39.65	105.92	-39.99
-0.1200.10-1	121.0	-39.66	110.35	-39.92
-0.1400.10-1	121.0	-39.66	114.99	-39.85
-0.1600.10-1	121.0	-39.66	119.43	-39.82

Table 8. Deviator stress and pore pressure with respect to vertical displacement in the case (ψ= 30°).

Displacement	Q8		SBT4	
	Deviator stress	pore pressure	Deviator stress	pore pressure
-0.2000.10-2	29.90	-9.804	29.70	-13.14
-0.4000.10-2	59.80	-19.61	59.40	-26.27
-0.6000.10-2	89.71	-29.41	89.09	-39.41
-0.8000.10-2	119.6	-39.22	108.37	-34.73
-0.1000.10-1	129.9	-29.60	123.59	-28.86
-0.1200.10-1	143.9	-23.63	139.13	-23.26
-0.1400.10-1	157.0	-16.83	154.99	-17.70
-0.1600.10-1	170.3	-10.22	171.03	-12.18

4. Conclusion

In this study, a four nodes triangular membrane finite element based on the strain approach having the two translations at each node (SBT4) is formulated for the static, nonlinear and free vibration analysis.

This type of strain-based element was implemented into the commercial code ABAQUS using the user element subroutine (UEL).

Several tests were considered as validation tests in this study, and the obtained numerical results were compared to known analytical or numerical solutions from the literature as well as some elements of ABAQUS.

Based on the numerical results of the problems tested, the present element SBT4 shows satisfactory agreement when compared with other robust elements.

Appendix

For the case of plane stress problem, the elasticity matrix [D] is:

$$[D]=\frac{E}{(1-\nu^2)}\begin{bmatrix} 1 & \nu & 0 \\ \nu & 1 & 0 \\ 0 & 0 & \frac{1-\nu}{2} \end{bmatrix}$$

For the case of plane strain problem, the elasticity matrix [D] is:

$$[D]=\frac{E}{(1+\nu)(1-2\nu)}\begin{bmatrix} (1-\nu) & \nu & 0 \\ \nu & (1-\nu) & 0 \\ 0 & 0 & \frac{(1-2\nu)}{2} \end{bmatrix}$$

[1] References

[2] Ashwell , D.G., Sabir, A.B. and Roberts, T.M. (1971), “Further studies in the application of curved finite elements to circular
[3] arches”, International Journal of Mechanical Sciences, vol.13, pp. 507–517.
[4] Sabir , A. B. (1985a) , “A rectangular and triangular plane elasticity element with drilling degrees of freedom”, Proceeding of
[5] the 2nd International Conference on Variational Methods in Engineering . Southampton University , Springer – Verlag,
[6] Berlin, pp.17-25.
[7] Belarbi , M.T ., Maalam , T. (2005) , “On improved rectangular finite element for plane linear elasticity analysis”, Rev . Eur.
[8] Elém.Finis, vol.14,pp.985-997.

[9] Rebiai , C ., Belounar, L. (2013), "A new strain based rectangular finite element with drilling rotation for linear and nonlinear
[10] analysis", Archive of civil and mechanical engineering, vol.13,pp.72-81.
[11] Rebiai,C., Belounar, L. (2014), "an effective quadrilateral membrane finite element for plate bending analysis",Measurement,
[12] vol.50,pp.263-269.
[13] Rebiai, C., Saidani, N and Bahloul, E. (2015), "A New Finite Element Based on the Strain Approach for Linear and Dynamic
[14] Analysis", Research Journal of Applied Sciences, Engineering, and Technology, vol.11,pp.639-644.
[15] Belarbi , M .T ., Bourezane, M. (2005), "On improved Sabir triangular element with drilling rotation", Rev. Eur. Genie Civil,
[16] Vol.9,pp.1151-1175.
[17] Hamadi,D.,Ayoub,A. And MaalemT. (2006a), "A new strain-based finite element for plane elasticity problems", Engineering
[18] Computations, Vol. 33, pp.562-579.
[19] Belarbi,M.T., Charif A.(1999), "Développement d'un nouvel élément hexaédrique simple basé sur le modèle en déformation
[20] pour l'étude des plaques minces et épaisses". Rev. Eur. Elém. Finis, vol.8, pp.135-157.
[21] Belounar , L., Guerraiche K ., (2014), "A new strain based brick element for plate bending", Alexandria Engineering Journal,
[22] vol.53, pp.95–105.
[23] Messai A., Belounar L., Merzouki T., (2019), "Static and free vibration of plates with a strain based brick element", European
[24] journal of computational mechanics, vol.99,pp.1-21.
[25] Sabir , A.B., Lock, A.C., (1972) , " A curved cylindrical shell finite element ". Int. J. Mech. Sci, Vol.14 , pp . 125 - 135.
[26] Assan , A. E., (1999), "Analysis of multiple stiffened barrel shell structures by strain-based finite elements". Thin-walled
[27] structures, vol.35,pp.233-253.
[28] Djoudi, M.S., Bahai , H. (2003) , "A shallow shell finite element for the linear and nonlinear analysis of cylindrical shells".
[29] Engineering Structures, Vol.25,pp.769-778.
[30] Djoudi , M.S., BahaiH., (2004a), "A cylindrical strain - based shell element for vibration analysis of shell structures". Finite
[31] Elements in Analysis and Design, Vol. 40, pp.1947-1961.
[32] Djoudi , M.S., BahaiH., (2004b), " Strain – based finite element for the vibration of cylindrical panels with openings". Thin-
[33] walled structures, vol.42,pp.575-588.
[34] Sabir , A.B, Moussa , A.I., (1996), "Finite element analysis of cylindrical-conical storage tanks using strain- based elements".
[35] Structural Engineering Review, vol.8,pp.367-374.
[36] Sabir , A.B., Moussa, A.I., (1997) , " Analysis of fluted conical shell roofs using the finite element method" Comput. Struct,

[37] Vol.64,pp.239-251.
[38] Mousa , A ., Djoudi , M . " New Strain - based Triangular Finite Element for the Vibration of Circular Cylindrical Shell with
[39] Oblique End". International Journal of Civil & Environmental Engineering IJCEE –IJENS, Vol.15, pp.6-11.
[40] Hamadi, D., Ayoub , A. And Ounis, A. (2015), "A new flat shell finite element for the linear analysis of thin shell structures".
[41] European Journal of Computational Mechanics, Vol.24, pp.232-255.
[42] Belounar, L., Guenfoud ,M., (2005), "A new rectangular finite element based on the strain approach for plate bending", Thin-
[43] Walled Structures, Vol.43,pp.47–63.
[44] Himeur , M ., Guenfoud , M .(2011) ," Bending triangular finite element with a fictitious fourth node based on the strain
[45] approach". European Journal of Computational Mechanics, Vol.20, pp.455 -485.
[46] Belounar, A., Benmebarek , S. and Belounar L., (2018), " Strain based triangular finite element for plate bending analysis".
[47] Mechanics of advanced materials and structures, doi.org/10.1080/15376494.2018.1488310.
[48] SabirA.B.,(1985b), "A segmental finite element for general plane elasticity problems in polar coordinates". Proceeding of the
[49] 8th International Conference Structure Mechanics in Reactor Technology. Belgium.
[50] Bouzrira, C., Sabir A.B., Nemouchi, Z.(2005), "A sector in-plane finite element in polar coordinates with rotational degree of
[51] freedom", Archives of civil engineering, Vol.51, pp.471-483.
[52] Bouzriba ,A., Bouzerira , C., (2015), "Sector element for analysis of thick cylinders exposed to internal pressure and change
[53] of temperature", Gradevinar, Vol.67, pp.547-555.
[54] Khiouani , H.E., Belounar , L. And Nabil Houhou M., (2020), " A New Three - Dimensional Sector Element for Circular Curved Structures Analysis". Journal of Solid Mechanics,Vol.12,pp.165-174
[55] MacNeal, R.H., Harder, R.L., (1985), "A proposed standard set of problems to test finite element accuracy". Finite Element
[56] Anal.Des, Vol.1, pp.3-20.
[57] Pian, T. H., Sumihara , K., (1984) , " Rational approach for assmed stress finite elements", IJNME, Vol. 20, pp.1685-1695.
[58] Cook, R.D., (1986) , "On the Allman triangle and a related quadrilateral element". Computer and Structure, Vol.22, pp.1065-
[59] 1067.
[60] Yanus,S.M.,Saiga,lS and CookR.D., (1989),"On improved hybrid finite element with rotational degrees of freedom", IJNME,
[61] Vol.28, pp.785-800.
[62] McNeal, R.H., Harder, R.L, (1988), " A refined four - noded membrane element with rotational degrees of freedom". C.S,
[63] Vol.28, pp.75-84.

[64] Sze, K.Y., Chen, W and Cheung, Y.K,(1992), "An efficient quadrilateral plane element with drilling degrees of freedom using
[65] orthogonal stress modes". ComputStruct, Vol.42, pp.695–705.
[66] Felippa, C.A., (2003) , "A study of optimal membrane triangles with drilling freedoms". Computer Methods in Applied
[67] Mechanics and Engineering, Vol.192, pp.2125–2168.
[68] Choo , Y.S., Choi , N. And Lee, B.C., (2006), "Quadrilateral and triangular plane elements with rotational degrees of freedom
[69] based on the hybrid Trefftz method". Finite Elements in Analysis and Design, Vol.42, pp.1002–1008.
[70] DaiK.Y., LiuG.R.,(2007), "Free and forced vibration analysis using the smoothed finite element method (SFEM) " ,Journal of
[71] Sound and Vibration, Vol,301, pp.803–820.
[72] Smith , I.M., Griffith, D.V., (2004), " Programming the Finite Element Method , 4th edition"., John Wiley & Sons, Ltd, UK
[73] Fortas, L., Belounar, L., & Merzouki, T. (2019). Formulation of a new finite element based on assumed strains for membrane structures. International Journal of Advanced Structural Engineering, 11, 9–18.
[74] Fortas Lahcene, Messai Abderraouf, Merzouki Tarek, Mohammed Sid Ahmed Houari (2022). Elastic stability of functionally graded graphene reinforced porous nanocomposite beams using two variables shear deformation. Steel and Composite Structures, , 43 (1), pp.31-54.